J. Condensed Matter Nucl. Sci. 13 (2014) 411–421

Research Article

Use of D/H Clusters in LENR and Recent Results from Gas-Loaded Nanoparticle-type Clusters

George H. Miley*, †, Xiaoling Yang, Kyu-Jung Kim, Erik Ziehm, Tapan Patel, Bert Stunkard and Anais Ousouf

Department of Nuclear, Plasma and Radiological Engineering, University of Illinois at Urbana-Champaign, IL 61801, USA

Heinrich Hora

Department of Theoretical Physics, University of New South Wales, Sydney, Australia

Abstract

Anomalous heat, attributed to Low-energy Nuclear Reactions (LENRs), is obtained by pressurizing metal alloy nanoparticles with deuterium gas. The reactions are enhanced by creation of ultra-high density deuterium clusters in the nanoparticles. Experiments comparing various nanoparticles and plans for a proof-of-principle unit are presented.
 ISSN 2227-3123

Keywords: Gas-loading system, Low-energy nuclear reaction, Nanoparticles

1. Introduction

Our previous experimental results have demonstrated the formation of ultra-high density hydrogen/deuterium nanoclusters with 10^{24} atom/cm [3] in metal defects (Fig. 1) [1,2,4–6]. Both experimental [7–11] and theoretical studies [12] have demonstrated that due to the close distance (ca. 2.3 pm) [7] between ions in the cluster, they can easily be induced to undergo intense nuclear reactions among themselves and some neighboring lattice atoms. In view of their multi-body nature, such reactions are termed Low-energy Nuclear Reactions (LENRs) – a terminology generally accepted by workers in the cold fusion field. Because the interacting ions have little momentum, the compound nucleus formed in these reactions is near the ground state so few energetic particles are emitted from its decay. Triggering excess heat generation, i.e., heat generation from nuclear reactions, in LENR experiments has been accomplished in various ways, all involving the loading of protons or deuterons into a solid metal or alloy material.

*E-mail: ghmiley@illinois.edu
†Also at: Lenuco LLP, Champaign, IL 61821, USA.

 ISSN 2227-3123

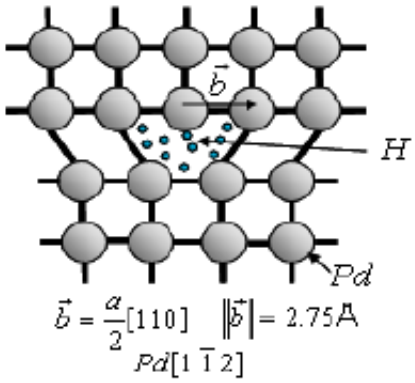

Figure 1. Scheme of edge dislocation loops in Pd containing.

Electrochemical loading was the initial approach of the experiment, and remains the most practiced approach. Gas loading is also widely used [13–23]. It is currently gaining more attention due to its smaller heat capacity and thereby higher temperature change as compared to an electrolysis system. In addition, a gas can be easily heated to temperatures greater than 100°C without excess pressure production. Therefore, the excess energy production from a gas-loading system can be observed more efficiently and in a relatively higher temperature range, making the technology compatible with existing energy conversion methods. Although the nuclear physics of LENRs is independent of the loading method, advantages of the gas-loading system described above using Ultra-High Density Deuterium (UHD-D) clusters can be taken advantage of to move the field towards a practical power unit. In this study, we report the anomalous heat generated from metal alloy nanoparticles loaded with deuterium through pressurizing the sample chamber.

Our gas-loading system is based on the design we first developed for thin film studies in 2010. Figure 2 shows the setup. Inside the large outer chamber (8-inch diameter) shown in Fig. 2(A) is a much smaller cylindrical pressure chamber (1-inch diameter), shown in Fig. 2(C). This arrangement uses a vacuum between the two cylinders to minimize heat losses and also provided a basis for measurement of heat flow for the calorimeter measurement. The nanoparticles are placed in the smaller chamber and loaded with deuterium (D_2) or hydrogen (H_2) gas. Three thermocouples are attached to the small cylinder – two at the sides and one at the bottom – to record the temperature during the loading and unloading process. The experiments described here used D_2 gas and Pd rich nanopartices. Other work with H_2 uses Ni-rich nanoparticles. A cold trap is connected between the smaller cylindrical chamber and the D_2 gas cylinder in order to provide extra purification for the flowing D_2 gas. During the D_2 gas loading and unloading process, the large chamber remained under a vacuum to reduce heat losses. The remaining heat loss is predominantly by radioactive heat transfer which can be calculated for calorimetric purposes from the thermocouple data. Figure 3 provides a further explanation of the operation of this gas-loading system.

Initial experiments with this system employed a “dynamic” loading where the system is first rapidly pressurized and after about 500 s depressurized. This is intended to study the initial adsorption effect, followed by desorption. The results shown in Fig. 4 loaded high purity D_2 gas at 60 psi into 20 g of Pd-rich nanoparticle powder (termed #1 nanoparticles). Figure 4 shows the raw data of this dynamic experiment – the temperature profiles shown recorded by three thermocouples attached to different locations on the sample cylinder. The slower increase of the temperature in two of the three thermocouples was later attributed to a poor connection to the cylinder surface. The initial rapid D_2 gas pressurization caused the temperature increase from ca. 20°C to ca. 50°C which produced ca. 1480 J energy

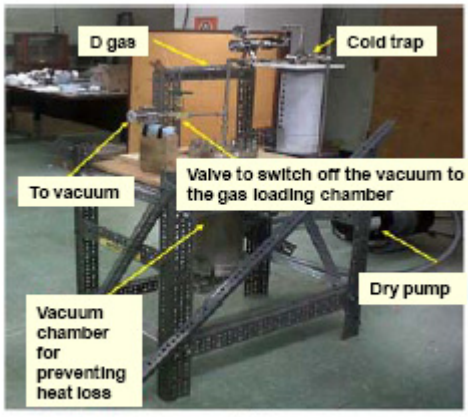

(A)

(B)

Diameter = 1 inch
Length = 3.69 inch,
Volume = 47.5 cm^3

(C)

Figure 2. (A) Gas-loading system, (B) students working on the system and (C) sample cylinder that contains nanoparticles in (B).

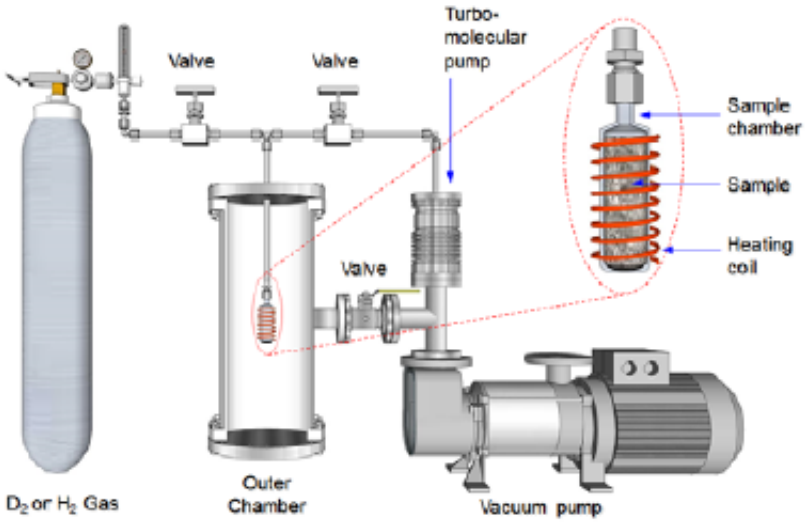

Figure 3. Sketch of the gas-loading system.

release, and is well above the exothermal energy 690 J that is calculated as the maximum possible from chemical reactions involving hydrating. (Note that the total heating energy was calculated by considering the heat capacity of both the sample cylinder and the nanoparticle powder, and the chemical exothermal energy was calculated using $\Delta H = \sim$35,100 J per mole of D_2 for the formation of PdD_x for $x < 0.6$.) The further rise in temperature from ca. 50°C to ca. 140°C during unloading D_2 gas is important because it is opposite from what would occur normally as deloading is an endothermic process. Thus, the heating is thought to be due to LENRs that are enhanced because of the increased deuterium flux inside the nanoparticles. However, more experiments are needed to eliminate side reactions such as oxygen and deuterium reactions. In this experiment, the input power, including power consumed by gas compression process and vacuum pumping process, is negligible compared to the output power. For example, considering the pumping process, the whole system can reach ca. 10^{-2} Torr within one minute. The volume of the sample chamber is less than one percent of the whole system, thus the power needed for vacuum pumping is negligible. The exact power used for gas compression is difficult to determine exactly, but calculation of the energy required is approximated by the power required to compress deuterium. Although many more studies are needed to unveil the source of the excess heat during the first step rise in temperature shown in Fig. 4, this result has provides evidence of significant excess energy gain [(Total energy out – energy in)/energy in]. In this short run the gain is already >1.0. Since the input energy is mainly due to exothermal heating during adsorption of the gas into the nanoparticles at the beginning of the run, the gain can be significantly increased by longer run times. Some data from such runs is shown next.

2. Parametric Gas-Loading Nanoparticle Experiments

We have performed various experiments to study the effect of changing some key parameters and to study longer run times. Each run involves loading and de-loading deuterium gas into nanoparticles by pressurizing and vacuuming

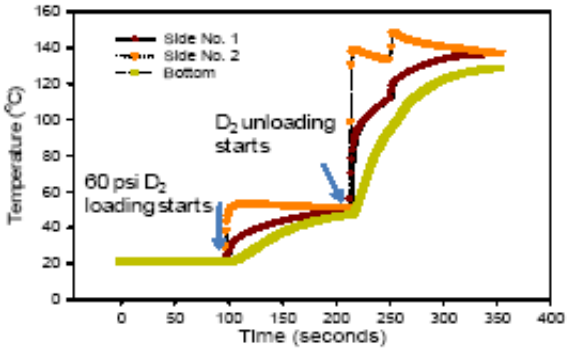

Figure 4. Raw data (temperature profile) from the dynamic experiment of the gas-loading system. The purpose of this very short dynamic run was to demonstrate the rapid temperature rise following a sharp pressure rise and the same upon sudden depressurization.

the sample cylinder. Two sets of different particles were used. The temperature profile for 23 g of nanoparticle #1 (same as in the dynamic run of Fig. 4) during the 60 Psi deuterium loading is shown in Fig. 5. We can see that the temperature rises right after gas- loading starts. The increasing rate is low at the start, but then exponentiates until reaching ca. 115°C. The initial slow rise is attributed to exothermal heating during the loading process, while the fast rise is attributed to LENRs. This is consistent with the theory that the LENRs are instated once a certain threshold temperature is reached. The temperature rising phase lasts about half an hour and then begins to decrease. The total energy produced in this 4.2-hour run was ca. 4770 J. The maximum exothermic energy from chemical reactions is calculated to be 690 J, suggesting the LENRs dominated with a gain (LENR energy out/Chemical energy in) of ∼6. This is viewed to be conservative. For example, if the calculation was based on the observed desorption energy, the value will be roughly twice of the above value (the value is quoted later in Table 1 using the latter technique). In this run, the averaged power density about 15 W/g.

The run in Fig. 5 was followed by another three runs using the same set of #1 nanoparticles. Figure 6 shows the

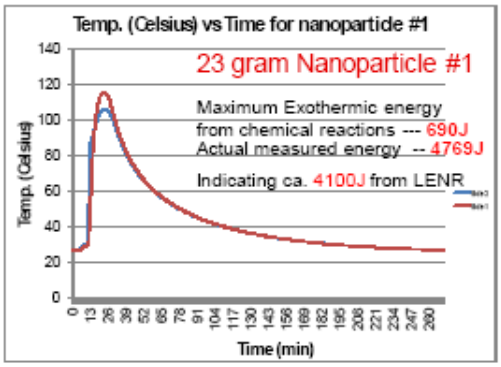

Figure 5. Temperature profile during the 60 Psi deuterium loading of the #1 nanoparticles. Two different curves were recorded by two thermocouples attached to the sample cylinder at different sites. In this case, 99.99% deuterium gas was used.

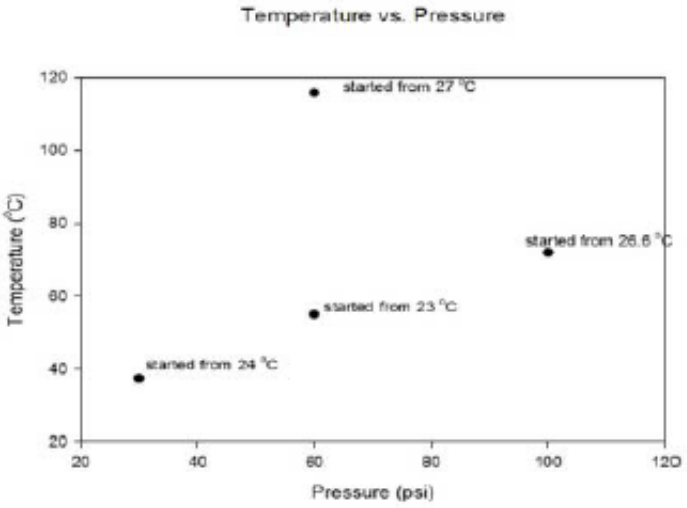

Figure 6. Temperature versus pressure for #1 nanoparticles. The one data point at the highest temperature is from fresh nanoparticles, whereas the other data are from the same particles after using first run.

peak temperature versus pressure for these runs. These three runs all have relative low temperature rises compared with the first run, but the three rises follow a linear relationship. The decreased temperature rise in the latter runs suggests the nanoparticles may be deteriorating, or sintering due to repeated use.

Figure 7 shows a SEM image of #1 nanoparticles before (Fig. 7(A)) and after (Fig. 7(B)) deuterium loading experiments. We can see that after deuterium loading, some nanoparticles, especially at the top layer, stick together compared with their loose-packed state before deuterium loading. The sintering of the layer may be blocking the deuterium gas from effectively going further into nanoparticles below the top layer, causing a lower temperature rise in the repeated experiment runs with the same packed nanoparticles. The sintering seems to occur at a lower temperature than expected, but hot spots may be caused by the localized loading cluster reactions. It is difficult to tell from the SEM image if there are any melted spots, but such local heating should not be neglected.

Following the experiment summarized in Fig. 6, improvements were made in nanoparticle manufacturing to provide much smaller size. In this case, three different alloys were employed for the nanoparticles, Type A is Pd rich similar to Type #1 used earlier, Types B and C contain both Pd and Ni, but with different percentages, along with small percentage of additional metals. As shown in following data, these new nanoparticles are much more reactive than that shown in Fig. 5. Table 1 lists a series of experiments performed to compare various types of nanoparticles. For these runs the outer vacuum chamber shown in Fig. 2 was removed and smaller weight of nanoparticles was employed in order to save total experiment time. A set of runs for the Type A nanoparticle is shown in Fig. 8. Only the initial run times up to 100 s from start of pressurization are analyzed for the comparisons. Note that with the decreased weight of nanoparticles used here and the faster heat loss due to the outer chamber removal, the temperature increase phase is much shorter than that in the runs of Fig. 5. As our main purpose for these experiments is to determine the best nanoparticles and to overcome sintering problems, the current adiabatic conditions with outer chamber removed are acceptable for such short times. Moreover, due to the fast heat loss, the analysis of the data is only done for the period of temperature increase as shown in Fig. 8. Three different types of nanoparticles (Types A–C) were employed in the comparison. Some were reused, either with or without treatment, following initial use. This was done to study the effect of sintering

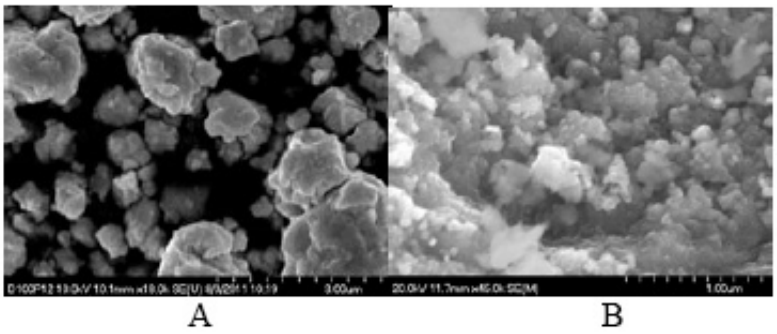

Figure 7. SEM image of the #1 nanoparticles before (A) and after (B) the deuterium loading experiment. Note: The white color in (B) is because the distance of the nanoparticles to the electron gun is different. The closer, the brighter. Also note that the nanoparticles employed in the adiabatic experiments described here are considerably smaller than those shown here.

and possible treatment of sintered particles. As seen in Table 1, the highest gain achieved (LENR energy out/estimated maximum possible chemical energy in) was 15.1 using Type C nanoparticles. The gain in these new sets of experiments more than doubled compared with previous ones due to the improved procedure of making nanoparticles. Note that this gain was achieved in only 98 s of the run. Since the adsorption (chemical) energy release occurs at the beginning of the run and then ends, longer runs than employed for these comparisons can give gains of many thousands. The highest power density achieved was 42.7 W/g using Type A particles. This is largely due to the rapid heating achieved with these particles (about 10 s to the peak vs.70–100 s for other particles.) Runs 2 and 6 used the same nanoparticle employed in Runs 1 and 5, respectively. Both suffered a significant reduction in performance, e.g. gains reduce roughly an order of magnitude. This is attributed to sintering effects caused in the initial run, even though it was fairly short.

However, results from run 3 suggest that the sintering problem seems solvable. In this run, particles from Run 2 were treated by reheating in the air for 2 h. When these particles were run they were able to release energy of 426 J/g, only 3% less than that achieved by the fresh particles in Run #1. This is very encouraging, and we are continuing study of ways to treat (added coatings, etc.) the nanoparticles to achieve longer initial runs prior to their re-treatment. Initial

Table 1. Adiabatic experiments for nanoparticle evaluation.

Run Nos.	Nanoparticle type	Gas	Pressure (Psi)	Mass (g)	Average ΔT (°C)	Joules (Peak)	Peak Energy /mass (J/g)	Run time - initial temp. to peak temp. (s)	W/g	Chemical energy (J)	Measured peak energy (J) minus chemical energy (J)	Gain
1	Type A	D_2	90	2.2	31.55	972.05	441.84	14.00	31.56	74.85	897.21	12.0
2	Type A (same particles from Run 1)	D_2	100	1.9	4.95	151.96	79.98	16.00	5.00	64.64	87.32	1.3
3	Type A (same particles as Run 2, but after heat treatment)	D_2	105	1.8	25.05	768.01	426.67	10.00	42.67	61.24	706.77	11.5
4	Type B	D_2	60	11.1	90.90	3588.88	323.32	95.00	3.40	271.29	3317.59	12.2
5	Type C	D_2	100	6.4	84.90	2754.00	430.31	98.00	4.39	170.76	2583.24	15.1
6	Type C (same particles from Run 5)	D_2	100	6.4	6.80	220.58	34.47	76.00	0.45	170.76	49.82	0.3
7	Type C	D2	100	3.2	27.10	846.04	264.39	78.00	3.39	85.38	760.66	9.3

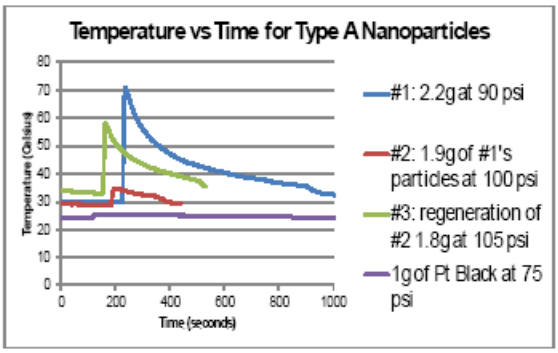

Figure 8. Typical adiabatic experiment with Type A nanoparticles. Included is a Pt black reference run data from these runs as well as others for different nanoparticles is summarized in Table 1.

results seem promising, but much more study and long run experiments are required to fully evaluate long run time issues.

To investigate possible gas impurity effects, another deuterium loading and unloading run followed using the same nanoparticles but low-purity (99.7%) deuterium gas at 60 Psi. The temperature only raised to ca. 30°C, suggesting excess heat production might be affected by the purity of deuterium gas. More study is needed, though, to confirm this and to identify the impurities involved that affect the reaction rate. This result also indicates that the heat from other reactions, such as a catalyzed deuterium oxidation reaction, is not a dominant reaction in the heat production process.

3. Comparison of Energy Output to other Power Sources

So far, our experiments suggest a remarkable proof-of-principle power unit at ca. 40 W/g, when using deuterium gas. This projection is based on the assumption that with an appropriate control system, the gas-loaded cell is able to maintain a steady-state temperature profile once it reaches the peak temperature.

This also requires nanoparticles with coating permitting long runs before removal for re-treatment. These methods are currently under study.

For perspective, it is useful to compare the envisioned LENR unit to a heat source such as Pu^{238} used for RTGs in NASA's deep space probes. Assuming a linear power/weight scaling, a 3-kW LENR unit (not including the gas tank) would use 0.5 kg or 0.3 L of nanoparticles compared to a 3-kW Pu^{238} unit which would be 5.6 kg or 0.28 L. However, this assumes the power obtained in the short LENR runs can be extended using control strategy and improve the nanoparticles as illustrated in Fig. 9. In that figure, the periodic oscillation pressure is employed to maintain the required flux in the nanoparticles giving a theoretical quasi-steady-state run. Note that the LENR data used is based on very preliminary experiments so improvements should be possible. Thus, it is foreseen that power densities for LENR can be expected to increase with further research development.

A new company, LENUCO has been set up in Champaign to commercialize this technology. The first goal is to develop units in the 1.5 kW_e range for house use. These would be stackable to form 30 kW_e units for small business applications. Thermoelectric energy conversion to electricity would be employed and the units would have cooling stream to allow use for co-generation operation. An earlier conceptual design for such a unit is shown in Fig. 10. While this design is for gas loading of thin films, it can easily be transformed to the device using nanoparticles.

Like other nuclear energy sources such as fusion and fission, a LENR cell offers a very high-energy density. However, LENR power sources offer other distinct advantages. Fission power faces limitations due to the need for

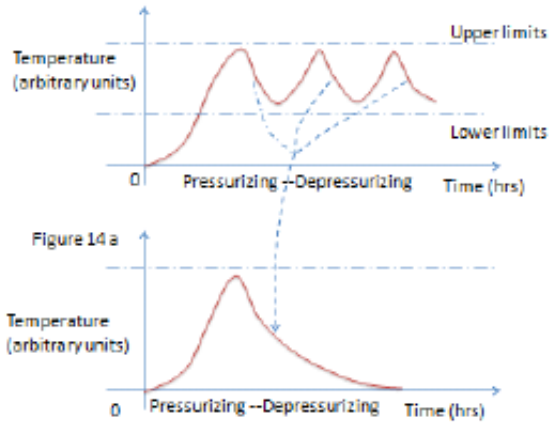

Figure 9. Illustration of pressure control to maintain flux of ions required for continuous long time operation. As seen once the temperature starts to decease, the pressure is reduced to initiate flow via desorption. These periodic pressure variations maintain a time-averaged temperature at the desired set-point.

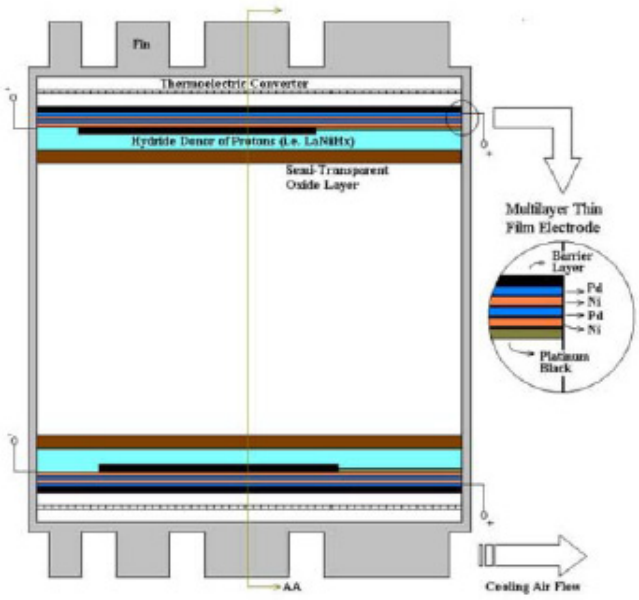

Figure 10. Conceptual design of a gas loaded thin film cell using thermoelectric energy conversion and air cooling. This base 1.5 kW_e module can be stacked to provide a 30 kWe unit for use in distributed commercial power units.

long-term storage of its radioactive waste. Fusion has less radioactivity involvement but with the planned initial use of D–T fuel still faces tritium containment issues and induced radioactivity of plant materials due to the intense flux of 14.7 MeV neutrons.

Also, scaling down to smaller power units is virtually impossible with these two nuclear sources. A LENR-based power source has reaction products that are mildly radioactive, mainly from low-energy beta decay from transmutation reactions. But with the short range of the betas, this radioactivity can easily be contained and quickly decays. The fuel it used, such as D_2, or H_2, is virtually inexhaustible. For LENR power sources, both scaling down and up in power are possible, and the huge energy released in the nuclear reactions (versus chemical reactions) makes this an extremely compact, long-lived energy source.

4. Conclusion

The primary result thus far is that the excess energies obtained in all experiments to date are all well above the maximum estimate of what could be attributed to chemical reactions. The external power/energy involved, such as deuterium gas compression and vacuum pumping, is minimal compared to the output, suggesting very large energy gain. This result is extremely encouraging relative to this gas-loaded cell becoming a remarkable power unit. The prime issue under study is to extend the run times using revised nanoparticle treatment combined with a pressure control to maintain a flux of ions in the nanoparticles following the initial loading. Finally optimization of the particle alloy and gas needs study involving the many system trade-offs. Along this line, our ongoing experiments are designed to compare Ni-rich-alloy-H2 with the present Pd-rich-alloy-D_2 system. Also, in order to understand the power scaling with pressure and weight of the nanoparticles, the earlier studies reported here need to be refined. In view of the many remaining issues at this point, it is premature to identify the best potential application. However, assuming the issues identified are resolved, numerous game-changing applications can be envisioned, for both space and terrestrial power. There are also numerous commercial uses on land, e.g. use in small power units for residential use including hot water heaters, use in larger power units for local power sources in commercial plants, and even DOD forward operating bases. Space applications, ranging from station keeping on to propulsion would also be revolutionized with such power units.

Acknowledgment

The support from New York Community Trust, NPL Associates Inc., and Lenuco is greatly appreciated.

References

[1] G.H. Miley and J.A. Patterson, Nuclear transmutations in thin-film nickel coatings undergoing electrolysis, *J. New Energy* **1**(3) (1996) 5.

[2] G.H. Miley, Product Characteristics and Energetics in Thin-Film Electrolysis Experiments, *Proc. Int. Conf. on Cold Fusion*, Vancouver, Canada, 1998, pp. 241–246.

[3] A. Lipson, B.J. Heuser, C. Castano, G.H. Miley, B. Lyakhov and A. Mitin, Transport and magnetic anomalies below 70 K in a hydrogen-cycled Pd foil with a thermally grown oxide, *Phys. Rev. B.* **72** (2005) 212507.

[4] A.G. Lipson, B.J. Heuser, C.H. Castano and A. Celik-Aktas, Observation of a low-field diamagnetic contribution to the magnetic susceptibility of deformed single crystal PdH_x ($x \simeq 4.0\times10^{-4}$), *Phys. Let. A* **339** (2005) 414–423.

[5] G.H. Miley, X. Yang and H. Hora, A potentially game changing green power source based on low energy nuclear reactions (LENRs), *Nuclear and Emerging Technologies for Space 2012*, The Woodlands, TX, March 19–23.

[6] G.H. Miley and X. Yang, Deuterium cluster target for ultra-high density, *18th Topical Meeting on the Technology of Fusion Energy*, San Francisco, CA, 2009.

[7] L. Holmlid, H. Hora, G. Miley and X. Yang, Ultra HIGH-DENSITY DEUTERIUM OF RYDBERG MATTER CLUSTERS FOR INERTIAL CON?NEMENT FUSION TARGETS, *Laser and Particle Beams* **27** (2009) 529–532.

[8] G.H. Miley, G. Narne, M.J. Williams, J.A. Patterson, J. Nix, D. Cravens and H. Hora, Multilayer thin-film microspheres after electrolysis, *Proc. Int. Conf. on Cold Fusion,* Vol. 2, edited by New Energy and Industrial Tech. Dev. Org., Japan, 1996, p. 529.
[9] A.G. Lipson, A.S. Rusetskii, A.B. Karabut and G.H. Miley, D–D reaction enhancement and X-ray generation in a high-current pulsed glow discharge in deuterium with titani um cathode at 0.8–2.45 kV, *J. Exp. and Theoret. Phys.* **100** (6) (2002) 1175–1187
[10] A.B. Karabut, A.G. Lipson and A.S. Roussetsky, Correct measurement of D–D reaction yield and in high current pulse-periodic deuterium glow discharge operating at 0.85–1.20 keV voltage applied, *Proc. 8th Int. Conf. of Cold Fusion,* Italy, 2000, p. 335.
[11] G.H. Miley, N. Luo, A.G. Lipson and A.B. Karabut, A Unique Plasma Discharge Driven Solid-State X-ray Laser, *SPIE Ablation*, Taos, NM, 2004.
[12] Y.E. Kim, Theory of Bose–Einstein condensation mechanism for deuteron-induced nuclear reactions in micro/nano-scale metal grains and particles, *Naturwissenschaften* **96** (2009) 803.
[13] Y. Arata and Y. Zhang, The establishment of solid nuclear fusion reactor, *J. High Temp. Soc.* **34** (2) (2008) 85.
[14] Y. Arata, Y. Zhang and X. Wang, Production of helium and energy in the 'solid fusion', 15^{th} *Int. Conf. Condensed Matter Nuclear Science*, Rome, Italy, 2009.
[15] Y. Sasaki et al., Anomalous heat generation in charging of Pd powders with high density hydrogen isotopes (i) results of absorption experiments using Pd powders, 15^{th} *Int. Conf. Condensed Matter Nuclear Science,* Rome, Italy, 2009.
[16] Y. Sasaki et al., Deuterium gas charging experiments with Pd powders for excess heat evolution (i) results of absorption experiments using Pd powders, *9th Meeting of Japan CF-Research Society*, Shizuoka, Japan, 2009.
[17] A. Takahashi et al., Deuterium gas charging experiments with pd powders for excess heat evolution (ii) discussions on experimental results and underlying physics, *9th Meeting of Japan CF-Research Society*, Shizuoka, Japan, 2009.
[18] A. Kitamura, T. Nohmi, Y. Sasaki, Y. Taniike, A. Takahashi, R. Seto and Y. Fujita, Anomalous effects in charging of Pd powders with high density hydrogen isotopes, *Phys. Lett. A* **373** (35) (2009) 3109–3112.
[19] D. Kidwell, Trace analysis of elements in a palladium matrix, *Int. Conf. Condensed Matter Nuclear Science*, Washington, DC, 2008, p.1.
[20] D. Kidwell et al., Does gas loading produce anomalous heat? *15th Int. Conf. Condensed Matter Nuclear Science*, Rome, Italy, 2009,p. 41 .
[21] F. Celani et al., Deuteron electromigration in thin Pd wires coated with nano-particles: evidence for ultra-fast deuterium loading and anomalous, large thermal effects, *Int. Conf. on Condensed Matter Nuclear Science,* Washington, DC, 2008, p.2.
[22] F. Celani et al., Towards a high temperature CMNS reactor: nano-coated Pd wires with D_2 at high pressures, *15th Int. Conf. on Condensed Matter Nuclear Science*, Rome, Italy, 2009, p. 25.
[23] X. Li et al., Progress in gas-loading D/Pd system—the feasibility of a self-sustaining heat generator, 10^{th} *Int. Conf. on Cold Fusion*, 2003, p.1.